THE *XMM-Newton* RGS SPECTRUM OF THE SEYFERT 1 GALAXY MARKARIAN 509

R.A.N. Smith*, M.J. Page, G. Branduardi-Raymont [a]

[a]Mullard Space Science Laboratory, UCL, Holmbury St. Mary, Dorking, Surrey RH5 6NT, England

We present an analysis of the soft X-ray spectrum of the Seyfert 1 galaxy Markarian 509 taken with the *XMM-Newton* Reflection Grating Spectrometer. We obtain values for the ionization, outflowing velocity and column density of three warm absorber phases along with the identification of two narrow and two broad emission lines.

1. Introduction

Soft X-ray absorption by ionized gas was first identified in Active Galactic Nuclei (AGN) by Halpern (1984) [1] and recent observations indicate that over half of Seyfert 1 galaxies may have these 'warm absorbers'. Gas properties are examined to improve our understanding of the kinematics, ionization and composition of these systems. The ionization parameter, ξ, determines the ionization state of the material and is defined as

$$\xi = \frac{L}{nr^2} \tag{1}$$

where L is the source luminosity (in $\mathrm{erg\,s^{-1}}$), n is the gas density (in $\mathrm{cm^{-3}}$) and r is the distance of the absorber from the centre of the system (in cm) (Tarter et al. 1969 [2]).

Markarian 509 is classified as a Seyfert 1 galaxy but is more like a Seyfert 1/quasi-stellar object (QSO) transition galaxy due to its compact appearance and high luminosity of $1.3 - 2.6 \times 10^{44}\,\mathrm{erg\,s^{-1}}$ in the 2-10 keV range (Weaver et al. 2001 [3]). Its close proximity, z=0.034397 (Fisher et al. 1995 [4]), compared to other AGN of similar luminosity, and the low Galactic column density in the line of sight ($\mathrm{N}_H = 4.4 \times 10^{20}\,\mathrm{cm^{-2}}$; Murphy et al. 1996 [5]), make it an ideal candidate for studying the inner regions of such objects.

2. Observations and Data Reduction

Our data were obtained with the Reflection Grating Spectrometer onboard the *XMM-Newton* observatory. The data analysed here are a combination of two observations of Markarian 509 by *XMM-Newton*. The first took place on 25 October 2000 with an exposure of 23.4 ks; the second took place on 20 April 2001 with an exposure time of 30.6 ks.

The data were processed using the *XMM-Newton* Science Analysis System (SAS) version 5.2. First and second order spectra from both RGS, and both observations, were extracted. To correct for residual artefacts in the effective area calibration (Stuhlinger et al. 2005 [6]), the effective area of each response matrix was divided by the ratio of a powerlaw + Galactic column fit to the *XMM-Newton* rev.0084 RGS spectrum of the continuum source Markarian 421. The Markarian 509 spectra and response matrices were resampled and coadded to produce a single spectrum and a single response matrix (Page et al. 2003 [7]). To improve signal to noise the data were grouped by a factor of 3, resulting in a spectrum with 1000 channels ~ 30 mÅ wide, well sampled with respect to the RGS resolution of ~ 70 mÅ FWHM. To correct for Galactic photoelectric absorption, the effective area elements of the response matrix were multiplied by the transmission as a function of energy for a column density of $4.4 \times 10^{20}\,\mathrm{cm^{-2}}$. Finally, the wavelength scale was transformed to the rest frame of Markarian 509. From this point onwards all data refer to the rest frame of the Markarian 509. The main software used to analyse the data was SPEX 2.00, a spectral fitting package created by J. S. Kaastra with high resolution X-ray spectra in mind.

2.1. The Continuum and Broad Emission Lines

We start by fitting the underlying continuum with a power law; however, there are regions where this is inadequate. The spectrum in Fig. 1

*E-mail: rans@mssl.ucl.ac.uk

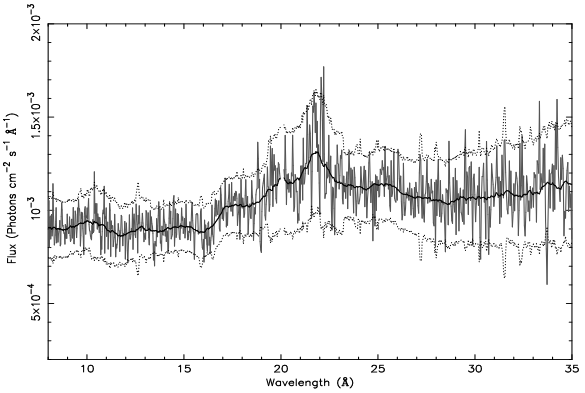

Figure 1. The RGS spectrum of Markarian 509 (grey), the smoothed continuum (black) and the 2σ error bounds (dotted), in the rest frame of the galaxy.

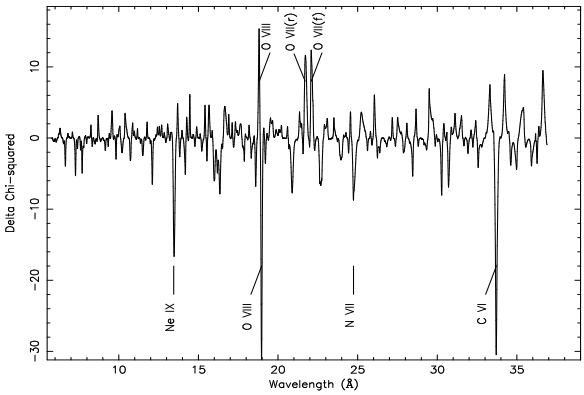

Figure 2. A graph of $\Delta\chi^2$ against wavelength to show the significant lines in the spectrum, in the rest frame of the galaxy.

shows broad peaks at 21.7Å and 25.2Å. There also appears to be a narrow emission feature either side of the C VI absorption line at 33.7Å (evident in Fig. 2), which can be fitted with a broad Gaussian line.

The broad emission lines at 21.7Å, due to O VII, and 33.7Å, due to C VI, give an average RMS velocity of 8000± 3000 km s^{-1} (Table 1). We identify the 25.2Å broad feature as a possible C VI radiative recombination continuum (RRC) similar to that observed in NGC4051 by Ogle et al.(2004) [8]. If this identification is correct then it would indicate a flow velocity of -820±3000 km s^{-1}. However, the identification of this feature is not sufficiently reliable to be retained in the spectral model, which comprises a power law and only two broad Gaussian emission lines at 21.7Å and 33.7Å.

The RMS velocity value of the C VI broad emission line suggests that it does not originate in any phase of the warm absorber, but is likely to arise in the broad line region of the AGN close to the centre of the system. This will also be the origin of the O VII triplet broad emission line, however, we cannot give a velocity profile as the broad fitted line is a combination of the three lines of the triplet. Kriss et al.(2000) [9] report broad O VI and C III emission lines with a FWHM of 11000 km s^{-1} in the UV spectrum of Markarian 509, a good match with our broad X-ray emission lines.

3. Narrow Emission Lines

We fit two significant narrow emission lines of O VII(f) and O VIII to the data: their RMS and flow velocities are listed in Table 1. The O VIII Lyα emission line has a much larger flow velocity than any other narrow emission line in the X-ray or UV spectra of Markarian 509. However, the O VIII absorption line, at 18.9Å, is likely to remove the long wavelength side of the emission line making it narrower and moving the peak to an apparently shorter wavelength.

The second narrow emission line included in our fit is the forbidden O VII line at 22.1Å. This is part of the O VII triplet and so other lines are to be expected, but these have been overshadowed by the broad O VII emission line centred at 21.7Å. Note the apparent flow velocities for our two narrow emission lines are significantly different (Table 1); this is likely to be due to both lines being confused by the presence of other emission and absorption lines and so it is still possible that these lines originate in the same region of the AGN and have the same velocity structure.

4. Absorption Profile

In order to analyse the absorption profile the data were fitted using the XABS component in SPEX 2.0. XABS applies absorption by photoion-

Table 1
Emission line parameters for both the broad (top) and narrow (bottom) fitted lines. No flow velocity is given for the O VII broad emission line due to the it being a combination of the three lines of the triplet.

Wavelength Å	FWHM Å	Norm 10^{50}ph s^{-1}	RMS Velocity km s^{-1}	Flow Velocity km s^{-1}	Transition
$21.67^{+0.19}_{-0.18}$	$0.63^{+0.32}_{-0.21}$	$11.0^{+2.1}_{-2.0}$	8700^{+1800}_{-2000}		O VII triplet
$33.72^{+0.29}_{-0.31}$	$0.80^{+0.55}_{-0.48}$	$4.0^{+2.4}_{-2.3}$	7100^{+4000}_{-3900}	-140^{+1800}_{-2400}	C VI Lyα
$18.82^{+0.10}_{-0.12}$	$0^{+0.33}_{-0}$	$1.1^{+0.5}_{-0.4}$	0^{+3200}_{-0}	-2400^{+250}_{-680}	O VIII Lyα
$22.12^{+0.13}_{-0.12}$	$0.13^{+0.26}_{-0.13}$	$2.4^{+0.7}_{-0.6}$	1700^{+2500}_{-1900}	$+360^{+550}_{-310}$	O VII(f)

Table 2
The XABS best fit parameters for a model including a power law, two broad and two narrow Gaussian emission lines and three XABS components, with the 2σ error bounds.

Phase	Flow Velocity km s^{-1}	RMS Velocity km s^{-1}	log ξ erg cm s^{-1}	N_H 10^{21}cm^{-2}	Prominent Ions
Phase 1	-510^{+290}_{-140}	0^{+20}_{-0}	$0.89^{+0.13}_{-0.11}$	$0.79^{+0.15}_{-0.13}$	O VI, N VI, Fe IX–Fe XIII
Phase 2	-260^{+120}_{-130}	70^{+70}_{-30}	$2.14^{+0.19}_{-0.12}$	$0.75^{+0.19}_{-0.11}$	O VII, N VII, C VI, Ne IX
Phase 3	-60^{+70}_{-200}	0^{+30}_{-0}	$3.26^{+0.18}_{-0.27}$	$5.5^{+1.3}_{-1.4}$	O VIII, Ne X, Fe XVII–Fe XX

ized gas, with variable column density, ionization parameter, elemental abundances, RMS velocity and flow velocity, to the power law plus emission lines model. In this way we are able to see if there are multiple phases in the gas and ascertain the parameters for each phase.

We have fitted the data with a number of XABS components with the abundances fixed at solar. The best fit (parameters in Table 2) suggests three distinct regions: a cool, high velocity phase producing the low ionization iron transitions forming the UTA at 16Å, along with the N VI and O VI absorption lines; the intermediate phase produces the C VI, N VII, Ne IX and O VII absorption lines, whilst the low velocity, high ionization phase produces the Ne X, O VIII and highly ionized iron absorption features.

Fig. 3 shows the best fit, which includes a power law, two broad emission lines, at 21.7Å and 33.7Å, two narrow emission lines, at 18.9Å and 22.1Å, and three XABS components with the parameters listed in Table 2.

Kriss et al.(2000) [9] and Kraemer et al.(2003) [10] identify carbon and oxygen as the main contributors to the UV absorption spectrum of Markarian 509. Interestingly we have found that a number of the UV absorbers identified have a similar outflow velocity to our Phase 1 and are also within the ionization range that this phase covers. We have used the ratios of the fluxes of these lines and the velocity profiles to find which phases are compatible and conclude that our Phase 1 is compatible with the UV Phase 2 from the Kraemer et al. and Kriss et al. analyses.

The analysis of Pounds et al. [11], whilst identifying an Fe M-shell UTA and NeIX absorption lines, finds no evidence of carbon or nitrogen absorption features and also appears to indicate an unusual ratio between the triplet lines. Pounds et al. identify two separate phases producing the RGS spectrum but do not give any values for the ionization parameters or column densities for us to compare with our analysis.

5. Conclusion

We present the most detailed analysis to date of the X-ray absorbing and emitting photoionized gas present in the Markarian 509 system using high resolution X-ray data from *XMM-Newton* .

The continuum has been fitted with a simple power law and three phases of photoionized gas: Phase 1 contains the high flow velocity, low ionization O VI and N VI absorption lines along

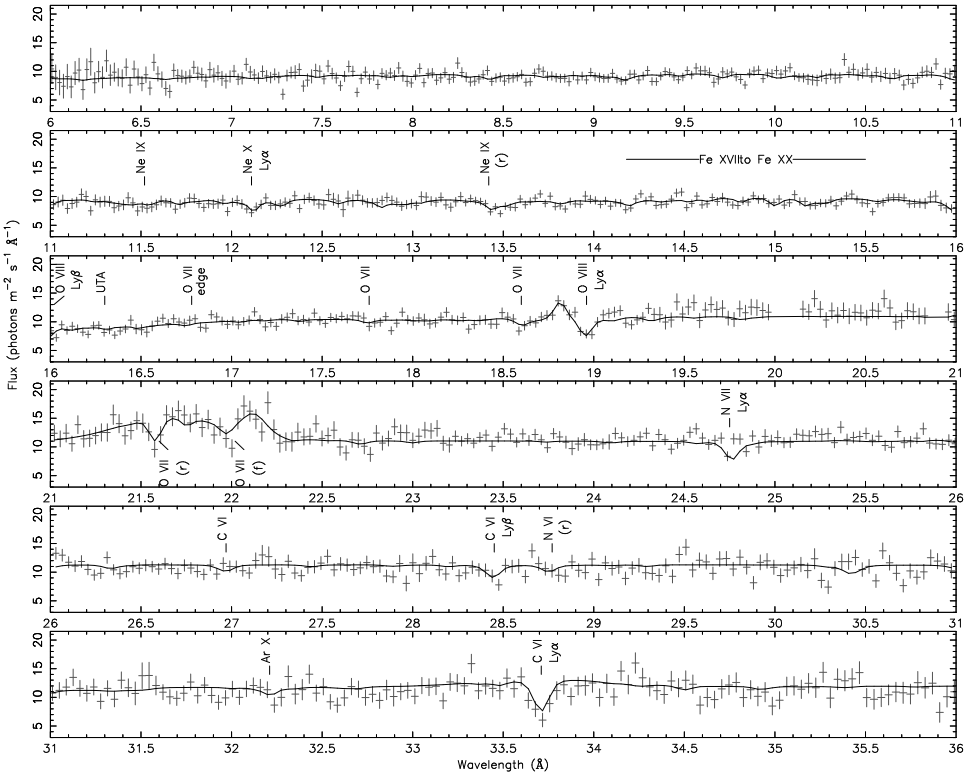

Figure 3. Markarian 509 RGS data fitted with a power law, three XABS components, two broad emission lines due to O VII and C VI and two narrow emission lines due to O VIII and O VII(f).

with an Fe M-shell UTA; Phase 2 contributes the medium ionization O VII, N VII, C VI and Ne IX absorption features, and Phase 3 produces the low flow velocity, high ionization O VIII, Ne X and highly ionized iron absorption features. However, we cannot rule out the possibility of a continuous ionization change throughout one gas system. We have identified Phase 1 as being compatible with a UV phase reported in previous studies.

We include two narrow emission lines due to O VII at 22.1Å, and O VIII at 18.8Å. We also identify two broad emission lines, due to O VII at 21.7Å, and C VI at 33.7Å, which have an RMS velocity of $8000\pm3000\,\mathrm{km\,s^{-1}}$ consistent with originating in the broad line region.

REFERENCES

1. Halpern, J.P., 1984, ApJ, 281, 90.
2. Tarter, C.B., Tucker, W.H., Salpeter, E.E., 1969, ApJ, 156, 943.
3. Weaver, K.A., Gelbord, J., Yaqoob, T., 2001, ApJ, 550, 261.
4. Fisher, K.B., Huchra, J.P., Strauss, M.A. *et al.* 1995, ApJ, 100, 69.
5. Murphy, E.M., Lockman, F.J., Laor, A., Elvis, M., 1996, ApJS, 105, 369.
6. Stuhlinger, M., Altieri, B., Esquej, M.P. *et al.* 2005, ESA SP-604, 2, 937.
7. Page, M.J., Soria, R., Wu, K. *et al.* 2003, MNRAS, 345, 639.
8. Ogle, P.M., Mason, K.O., Page, M.J. *et al.* 2004 ApJ, 606, 151.
9. Kriss, G.A., Green, R.F., Brotherton, M. *et al.* 2000, ApJ, 538, L17.
10. Kraemer, S.B., Crenshaw, D.M., Yaqoob, T. *et al.* 2003, ApJ, 582, 125.
11. Pounds, K., Reeves, J., O'Brien, P. *et al.* 2001, ApJ, 559, 181.